PNAS RESEARCH ARTICLE | PHYSIOLOGY

Bioengineered peptibodies as blockers of ion channels

Bojjibabu Chidipi[a,1], Mengmeng Chang[a,1], Meng Cui[b], Obada Abou-Assali[a], Michelle Reiser[a], Sergii Pshenychnyi[c], Diomedes E. Logothetis[b], Michael N. Teng[d,2], and Sami F. Noujaim[a,2]

Edited by Lily Jan, HHMI, University of California, San Francisco, CA; received July 21, 2022; accepted October 25, 2022

We engineered and produced an ion channel blocking peptibody, that targets the acetylcholine-activated inwardly rectifying potassium current (I_{KACh}). Peptibodies are chimeric proteins generated by fusing a biologically active peptide with the fragment crystallizable (Fc) region of the human immunoglobulin G (IgG). The I_{KACh} blocking peptibody was engineered as a fusion between the human IgG1 Fc fragment and the I_{KACh} inhibitor tertiapinQ (TP), a 21-amino acid synthetic peptidotoxin, originally isolated from the European honey bee venom. The peptibody was purified from the culture supernatant of human embryonic kidney (HEK) cells transfected with the peptibody construct. We tested the hypothesis that the bioengineered peptibody is bioactive and a potent blocker of I_{KACh}. In HEK cells transfected with Kir3.1 and Kir3.4, the molecular correlates of I_{KACh}, patch clamp showed that the peptibody was ~300-fold more potent than TP. Molecular dynamics simulations suggested that the increased potency could be due to an increased stabilization of the complex formed by peptibody-Kir3.1/3.4 channels compared to tertiapin-Kir3.1/3.4 channels. In isolated mouse myocytes, the peptibody blocked carbachol (Cch)-activated I_{KACh} in atrial cells but did not affect the potassium inwardly rectifying background current in ventricular myocytes. In anesthetized mice, the peptibody abrogated the bradycardic effects of intraperitoneal Cch injection. Moreover, in aged mice, the peptibody reduced the inducibility of atrial fibrillation, likely via blocking constitutively active I_{KACh}. Bioengineered anti-ion channel peptibodies can be powerful and highly potent ion channel blockers, with the potential to guide the development of modulators of ion channels or antiarrhythmic modalities.

peptibody | potassium channels | protein engineering | I_{KACh}

Significance

We report the bioengineering of a designer ion channel blocker that is potent and bioactive. This blocker is a fusion protein between the Fc fragment of the human IgG1 and a peptidotoxin (tertiapinQ) originally isolated from the venom of the honey bee. In the heart, this designer protein blocks a specific potassium current (I_{KACh}), could potentially be used as a platform for the study of ion channel function, and could even have therapeutic applications.

Highly potent ion channels blocking modalities are needed for the development of the next generation of antiarrhythmic pharmacotherapies (1). We engineered and produced an ion channel blocking peptibody, that targets the acetylcholine-activated inwardly rectifying potassium current (I_{KACh}).

Peptibodies are chimeras generated as fusion proteins of the fragment crystallizable (Fc) domain of the human immunoglobulin G (IgG) with a bioactive "warhead" peptide (2, 3). Peptibodies combine the biologic/therapeutic activity of a given peptide, with the stability of monoclonal antibodies. They are stable and safe molecules that are emerging as viable clinical therapeutics (2, 3). For instance, the first peptibody in clinical use is Romiplostim, which is approved for the treatment of immune thrombocytopenic purpura. Romiplostim is composed of thrombopoietin mimetic peptides fused to the C terminus of the Fc region of human IgG (4–8).

We engineered, produced, and characterized an ion channel blocking peptibody, constructed as a fusion protein between the human IgG1 Fc fragment and tertiapinQ (TP), a 21-amino acid synthetic peptidotoxin originally isolated from the European honey bee venom. In the heart, TP has been shown to inhibit I_{KACh} (9, 10).

Cardiac I_{KACh} is a current that flows through the tetrameric sarcolemmal channel formed by Kir3.1 and 3.4 protein subunits. Baseline I_{KACh} is minimal (11); however, parasympathetic stimulation results in direct activation of I_{KACh} via the βγ subunits of Gi, in a muscarinic (M2) receptor-dependent manner (12–15). In some forms of atrial fibrillation (AF), it was shown that I_{KACh} is constitutively active, behaves as a background potassium inward rectifier, and can thus contribute to the initiation and maintenance of the arrhythmia (16, 17). Since I_{KACh} is mainly expressed in the atria and is largely absent from the working ventricular myocardium, it has been proposed that blocking I_{KACh} can be an atrial-selective rhythm control pharmacotherapy (1, 16, 18).

Here, we describe the bioengineering and characterization of a peptibody that blocks I_{KACh}. We tested the hypothesis that in the heart, the engineered peptibody is a potent blocker of I_{KACh} in vivo and in vitro and serves as an antiarrhythmic. The goal being to demonstrate that peptibodies can be used as cardiac ion channel blockers and can also guide the generation of novel antiarrhythmic modalities.

Author affiliations: [a]Department of Molecular Pharmacology and Physiology, Morsani College of Medicine, University of South Florida, Tampa, FL 33612; [b]Department of Pharmaceutical Sciences, School of Pharmacy, Bouvé College of Health Sciences, Center for Drug Discovery, Northeastern University, Boston, MA 02115; [c]Chemistry for Life Processes Institute, Northwestern University, Evanston, IL 60208; and [d]Department of Internal Medicine, Morsani College of Medicine, University of South Florida, Tampa, FL 33612

Author contributions: M.N.T. and S.F.N. designed research; B.C., M. Chang, M. Cui, O.A.-A., M.R., S.P., D.E.L., M.N.T., and S.F.N. performed research; B.C., M. Chang, M. Cui, M.R., D.E.L., M.N.T., and S.F.N. analyzed data; and B.C., M. Chang, M. Cui, D.E.L., M.N.T., and S.F.N. wrote the paper.

Competing interest statement: The authors have patent filings to disclose. M.N.T. and S.F.N. have been granted patent number 11,014,971, issued by USPTO on 06/25/2021.

This article is a PNAS Direct Submission.

[1]B.C. and M. Chang contributed equally to this work.

[2]To whom correspondence may be addressed. Email: mteng@usf.edu or snoujaim@usf.edu.

Published December 7, 2022.

Results

Design, Expression, and Purification of the Peptibody. We designed the I_{KACh} blocking peptibody (Fc-TP) as a fusion protein between the human IgG1 Fc fragment (330 amino acids) and TP (21-amino acids), separated by a linker composed of eight glycines (Fig. 1*A*). TP is a 21-amino acid synthetic peptidotoxin originally isolated from the European honey bee venom, and in the heart, it has been shown to be a specific blocker of I_{KACh}. The N terminus of the peptibody contains an artificial leader sequence composed of 19 amino acids, that drives secretion of the peptibody. This configuration of the peptibody does not interfere with the C terminus of TP, since it has been suggested to be important for I_{KACh} block (19). The DNA sequence of the construct was synthesized and cloned into pcDNA3.1. The plasmid construct was then used to transfect human embryonic kidney (HEK293) cells. Since the peptibody contained an N-terminal leading sequence, the secreted peptibody was subsequently purified from the media via a mono-affinity A resin column. Fig. 1*B* shows sodium dodecyl sulfate-polyacrylamide gel electrophoresis (SDS-PAGE) gel (*Left*) and corresponding Western blot (*Right*) images of increasing amounts of peptibody and of Fc, under reducing conditions. The protein gel and the blot show the peptibody (Fc-TP) and recombinant Fc at about 40 KDa. We then calculated the half-life ($t_{1/2}$) of the peptibody injected via tail vein- 5.5 μg in 50 μl phosphate buffered saline (PBS)- in mice using an enzyme-linked immunosorbent assay (ELISA) based human Fc quantification assay (Fig. 1*C*). The peptibody half-life was 13 h, in line with published half-lives of Romiplostim, and human recombinant Fc in rodents (20, 21).

Effect on I_{KACh} Current. We tested in patch-clamp experiments, whether the peptibody inhibits I_{KACh} (Fig. 2). Barium-sensitive I_{KACh} currents were recorded in HEK293 cells stably transfected with Kir3.1/3.4 (15) at 50 mM extracellular K^+, in response to a 2-s ramp from −140 to +40 mV, from a holding potential of 0 mV (15, 22). These cells overexpressing Kir3.1/3.4 displayed a basal, non-stimulated I_{KACh} current (15). At 100 pM, while Fc (Panel *A*) and TP (Panel *B*) had minimal effects on I_{KACh}, the peptibody blocked the current significantly (Fc-TP, Panel *C*). The concentration-response curves of current block at −120 mV revealed that the peptibody was over 300 times more potent than TP. The IC_{50} of the peptibody was 24.9 pM, versus 9.06 nM for TP, and the naked Fc fragment did not block the current.

Molecular Modeling of I_{KACh} Block by the Peptibody. The peptibody showed an unexpected 300-fold increase in potency over TP. We thus used molecular modeling to explore the possible underlying mechanism. We developed homology models for the Kir3.1/3.4 channel that contain two Kir3.1 and two Kir3.4 subunits based on the crystal structure of Kir3.2 (PDBID: 3SYA). The Kir3.1/3.4 channel model with the best discrete optimized protein energy (DOPE) score was selected for molecular docking simulations to predict tertiapin–channel interaction. To account for the flexibility of tertiapin for the docking simulations, all 21 NMR conformations available (PDBID: 1TER) were docked. The top-ranked poses from the docking simulations were selected and subjected to ***molecular dynamics*** (MD) simulations to calculate binding free energies. Among all the predicted complexes of tertiapin-Kir3.1/3.4, the system with the lowest binding free energy is shown in Fig. 3*A*. The critical interactions between tertiapin and the channel are electrostatic salt bridges formed between the tertiapin C-terminal amino acids K20, K21, K17 and residue E131 in Kir3.4, as well as tertiapin R7 with Kir3.4 residue D123, and tertiapin K16 with Kir3.1 residue Y146 and with Kir3.4 residue Y152. We also plotted the distances of these salt bridges as a function of MD simulation time (100 ns) in Fig. 3*B*. Tertiapin residues K17 and R7 formed stable salt bridges with Kir3.4 residue E131 and D123, respectively, during the simulations (*Left-most* graph), while tertiapin residues K20 and K21 formed transient, unstable salt bridges with Kir3.4 residue E131 (*Middle* graph). Tertiapin residue K16 acted as a plug, forming a stable interaction with Kir3.1 residue Y146 and Kir3.4 residue Y152 of the channel.

Modeling the Interaction between the Peptibody and Kir3.1/3.4 Tetrameric Channels. To build the peptibody-channel complex, we generated a peptibody model using the I-TASSER website server. Then the two tertiapin molecules of the peptibody were replaced by two tertiapin-Kir3.1/3.4 model structures of Fig. 3,

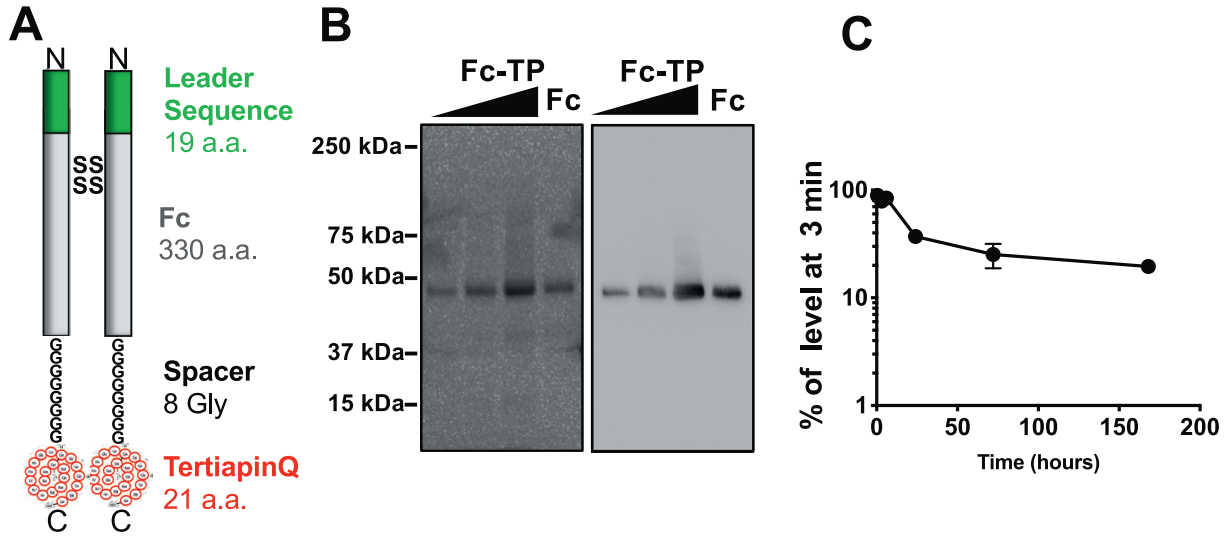

Fig. 1. Peptibody design and production. *A.* Cartoon of the peptibody. An artificial leader sequence (green) is at the N terminus, in order to ensure the secretion of the peptibody. Grey is the Fc fragment of the human IgG1, composed of 330 aminoacids followed by an octaglycine spacer, then by the 21 aminoacids TP. The peptibody is a dimer. Dimerization is via disulfide bonds formation (SS). *B.* Protein SDS-PAGE gel (*Left*), and its corresponding Western blot (*Right*) of increasing amounts of the peptibody (Fc-TP, 0.2, 0.4, and 1 μg), and recombinant Fc control. *C.* Pharmacokinetics analysis of the peptibody.

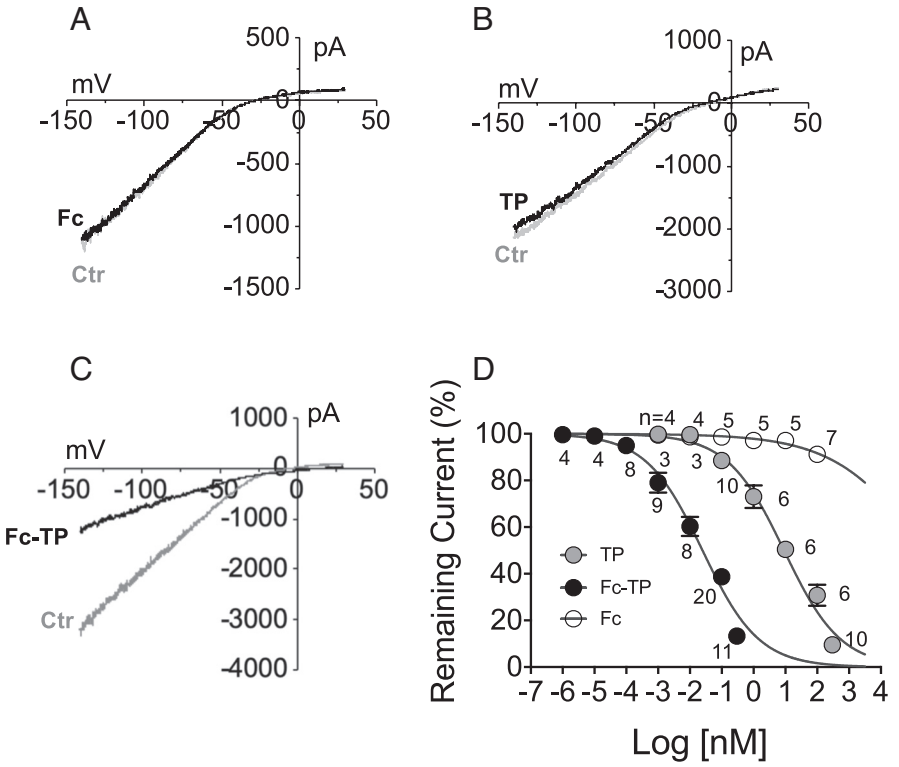

Fig. 2. Block of I_{KACh} by the peptibody in HEK293 cells stably transfected with Kir3.1 and Kir3.4. The current was elicited by a 2-s ramp from −140 mV to 40 mV. *A.* IV relationship of I_{KACh} in a cell at baseline (Ctr), and after addition of 100 pM human IgG1 Fc fragment. *B.* IV relationship of I_{KACh} in a cell at baseline (Ctr), and after addition of 100 pM TP. *C.* I–V relationship of I_{KACh} in a cell at baseline (Ctr), and after addition of 100 pM peptibody (Fc-TP). *D.* Concentration-response curve of I_{KACh} block by the Fc fragment, TP, and peptibody (Fc-TP). The number of cells at each tested dose is shown. The IC_{50} for TP block was 9.06 nM, and that for the peptibody was 24.9 pM.

using Discovery Studio software. Fig. 4 shows the peptibody-channel complex composed of a peptibody molecule interacting with two Kir3.1/3.4 channels (Fig. 4*A*). In order to estimate and compare free energies of the tertiapin and peptibody binding to the Kir3.1/3.4 channel, the tertiapin-Kir3.1/3.4 and peptibody-Kir3.1/3.4 systems of Figs. 3*A* and 4*A*, respectively, were immersed in an explicit membrane environment for 100 ns and MD simulations were carried out. Fig. 4*B* shows the root-mean-square deviation (RMSD) of alpha carbon atoms as a function of time from the two MD simulations. Both systems were equilibrated after 60 ns of simulation. Therefore, the last 40 ns were used for Molecular Mechanics-Generalized Born Surface Area (MMGBSA) binding free energy calculations. The binding free energies were −24.79 Kcal/mol for the tertiapin-channel system and −44.46 Kcal/mol for the peptibody-channel complexes, respectively. These simulations suggest that the significantly more potent peptibody's block of I_{KACh} compared to that of TP may be due to a lower free energy of binding due to the more stable interaction of the peptibody with the channel.

In Vivo Effects. Subsequently, we investigated in mice whether the peptibody displayed cardiac bioactivity by quantifying its effects on heart rate in anesthetized C57BL/6J mice (1.8% isoflurane), with continuous electrocardiogram (ECG) monitoring. Intraperitoneal (i.p.) administration of carbachol (Cch) (300 μL of 200 μM) caused a significant slow down of heart rate due to I_{KACh} activation (11) (Fig. 5*A*, first column: ECG at baseline control, *Middle* column: after Cch). The peptibody, Fc-TP, or the Fc fragment were delivered via jugular vein injection (5.5 μg in 50 μl PBS). At 7 min after delivery, Fc-TP reversed the bradycardic effects of Cch, while at the same dose Fc had a significantly less pronounced effect (Panel *A*, *Right* column). Panel *B* is a compilation of six mice injected with Fc, and five with the peptibody. The peptibody, but not the Fc fragment, significantly blunted the RR interval prolonging effects of Cch. We then tested how long a single injection of the peptibody is bioactive and thus affects heart rate in Cch-challenged mice. Seven mice received a single-tail vein injection of the peptibody (5.5 μg in 50 μl PBS), and seven animals were injected with Fc. The ECG was then recorded in the anesthetized animals during Cch challenge at 30 min after peptibody or Fc injection, then the challenge was repeated again at 48 and 72 h post-injection with the peptibody or Fc. At 48 h, the peptibody had significant effects (184.4 ms ± 14.9) versus Fc (254.9 ms ± 28.8) on the RR interval of Cch-challenged animals ($P < 0.05$, Student's t test).

Atrial Specificity. Since I_{KACh} is mainly expressed in atrial cells, we used whole-cell patch-clamping in isolated adult atrial and ventricular mouse cardiomyocytes to investigate whether the peptibody was atrial specific. Currents were recorded by holding at −40 mV for 100 ms, followed by 1,000 ms steps from −140 mV to +40 mV in 10 mV increments in 50 mM extracellular K^+. After recording baseline currents, the extracellular solution was exchanged to contain 20 μM Cch to activate I_{KACh}, followed by application of peptibody (Fc-TP), TP, or Fc. In Fig. 6*A*, the left tracings are the background currents recorded in response to voltage steps in an atrial myocyte. The middle tracings are the currents that increased in the presence of Cch, due to I_{KACh} activation. The right tracings show that addition of 100 pM peptibody blocked the Cch-activated I_{KACh}. The rightmost panel shows the superimposed IV curves of the barium-sensitive currents at baseline control, after activation with Cch, and after addition of the peptibody, which significantly reduced the Cch-induced I_{KACh}. In Fig. 6*B*, the current traces and the IV curves show that 100 pM

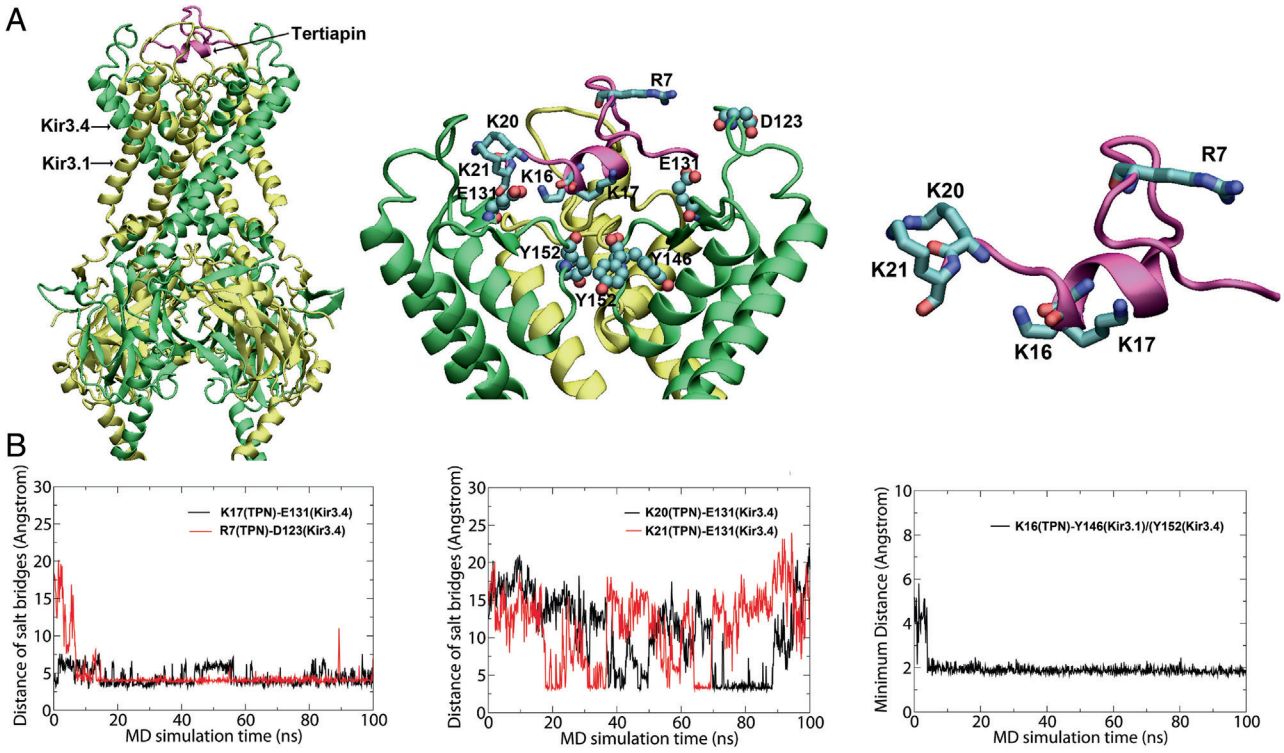

Fig. 3. Molecular modeling of the interaction between tertiapin and Kir3.1/3.4 channel. *A*. *Left*: Homology model of the heterotetrameric Kir3.1/3.4 channel bound to the tertiapin conformer resulting in the lowest binding free energy. *Middle*: Zoomed in view of the complex, with the front Kir3.1 subunit removed for clarity. The critical interactions between tertiapin amino acids (represented as sticks) and channel amino acids (represented as Van der Waals radii) are shown. The interactions are electrostatic salt bridges formed between amino acids K20, K21, K17 in tertiapin, and E131 in Kir3.4, R7 amino acid in tertiapin and D123 in Kir3.4, and K16 in tertiapin, and Y146 in Kir3.1 and Y152 in Kir3.4. *Right*: The conformer of tertiapin that produced the lowest binding free energy. *B.* The distances of the salt bridges of *A* as a function of MD simulation time (100 ns) are plotted. The interacting pair K17 in tertiapin and E131 in Kir3.4, and the pair composed of R7 in tertiapin and D123 in Kir3.4 form stable salt bridges during the simulations (*Left* plot), while the pairs K20 in tertiapin/E131 in Kir3.4, and K21 in tertiapin and E131in Kir3.4 form only transient (unstable) salt bridges (*Middle* plot). K16 in tertiapin acts as a plug residue interacting with Y146 in Kir3.1 and Y152 in Kir3.4 (*Right* plot).

TP did not block I_{KACh}. This demonstrates that at 100 pM, while the peptibody completely blocked I_{KACh}, TP did not have any effect. Therefore, in atrial myocytes as in transfected HEK293 cells (Fig. 2), the peptibody is a more potent blocker of I_{KACh} compared to TP. We then tested if the peptibody is atrial specific. In Fig. 6*C*, the left tracings are background currents recorded in response to voltage steps from −140 mV to 40 mV in a ventricular myocyte. The middle tracings are the currents which did not change in the presence of Cch in the bath solution. The third panel shows currents which also did not change in the presence of 100 pM peptibody. The last panel displays IV curves of barium-sensitive currents at baseline control, after Cch, and after the peptibody. The peptibody did not modify the barium-sensitive background current, i.e., I_{K1}, in ventricular myocytes, indicating that in the heart while the peptibody blocks I_{KACh}, it does not block other potassium inward rectifying currents such as I_{K1}.

Constitutively Active I_{KACh} in the Mouse Heart. The incidence of AF dramatically increases with age, and epidemiological studies have stablished a clear link between aging and AF (23). In fact, advancing age is one of the most significant risk factors for AF (23). While constitutively active I_{KACh} is important in persistent AF, it remains unclear if I_{KACh} is constitutively active in the aged heart and whether this can be one of the mechanisms that link the cardiac aging process with proarrhythmic changes in atrial membrane excitability. Since we are unaware of a mouse model of spontaneous AF where I_{KACh} is constitutively active, we conducted a series of experiments to investigate if I_{KACh} is constitutively active in the aged mouse heart, and if it can be blocked by the peptibody. We isolated atrial myocytes from young (3 to 5 mo), and aged (19 to 24 mo) C57BL/6J mice of both sexes, and used patch clamp to interrogate whether in aged atrial myocytes I_{KACh} is constitutively active, and can be blocked by the Fc-TP peptibody. In Fig. 7*A* are background current tracings from atrial myocytes of young mice according to the protocol described for Fig. 6. The top tracings are for baseline controls, and the bottom tracings are after addition of 100 pM Fc fragment or the peptibody (Fc-TP). Neither Fc nor the Fc-TP had effects. Panel *B* is IV curves of baseline, and Fc (*Top*) and baseline and Fc-TP (*Bottom*). In Panels *C* and *D*, the same experiment was repeated in atrial myocytes isolated from aged mice. In Panel *C*, the top tracings are for baseline controls, and the bottom tracings are after addition of 100 pM Fc fragment or the Fc-TP. The Fc fragment did not affect the current. However, Fc-TP significantly reduced the current, indicating block of constitutively active I_{KACh}. Panel *D* shows IV curves of Fc (*Top*) which did not block the background current in aged mice and Fc-TP (*Bottom*), which resulted in a significant reduction of the current, demonstrating that the peptibody blocks constitutively active I_{KACh} in aged atrial myocytes.

Antiarrhythmic Activity. Lastly, we investigated whether the peptibody displayed anti-AF activity in aged mice. We used in vivo atrial programmed electrical stimulation after jugular vein injection of the peptibody or the Fc fragment. The weight and age of animals injected with the peptibody were not different from those injected with Fc (Fig. 8*A*). In Fig. 8*B*, the top panel displays ECG (*Top*) and intracardiac electrogram (*Bottom*) tracings showing that burst pacing induced AF in an Fc-injected mouse,

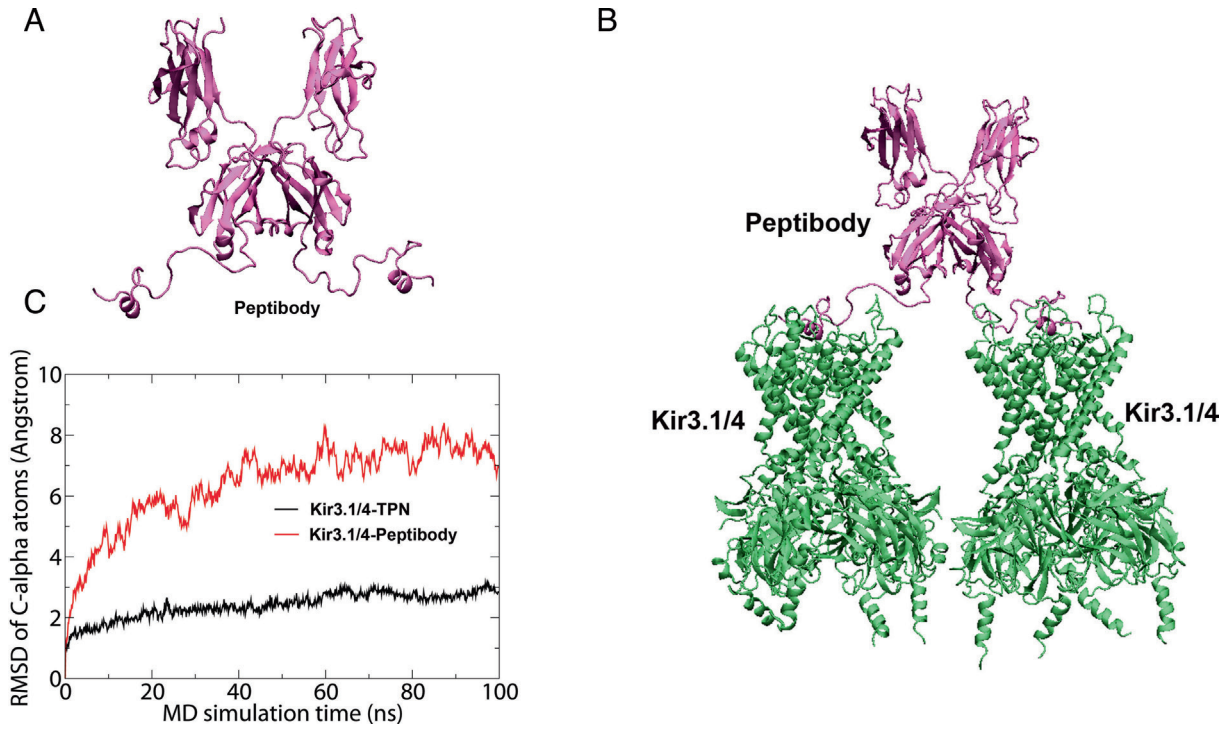

Fig. 4. Molecular modeling of the interaction between the peptibody and Kir3.1/3.4 channel. *A*. Peptibody model. *B*. Model of the complex formed by the peptibody and two Kir3.1/3.4 channels. The model of the complex was built based on the tertiapin-Kir3.1/3.4 channel interaction described in Fig. 4. The tertiapin sub-structural units in the peptibody were replaced by the predicted docking conformations of tertiapin bound to Kir3.1/3.4 channels. *C*. RMSD of alpha carbon atoms as a function of time from the MD simulations of tertiapin-Kir3.1/3.4, and the peptibody-Kir3.1/3.4 systems. Both systems were equilibrated after 60 ns simulations, and the last 40 ns simulations were used for binding free energy calculations. The binding free energies were −24.79 and −44.46 kcal/mol for the tertiapin-Kir3.1/3.4 and the peptibody-Kir3.1/3.4 complexes, respectively.

but not in a peptibody-injected mouse (*Bottom*). Panel *C* shows that AF was inducible in 100% (five out of five) of animals that received Fc, while 20% (one out of five) of animals treated with the peptibody were inducible for AF ($P < 0.05$, Fisher's exact test). Thus, the peptibody reduced AF inducibility in aged mice, likely via blocking constitutively active I_{KACh}.

Discussion

Our work demonstrates that bioengineered anti-ion channel peptibodies can be powerful and produce highly potent ion channel blockers. Peptibodies are safe and flexible alternatives to therapeutic antibodies (2, 3). The peptibody we engineered to block I_{KACh} was designed as a fusion protein between TP and the Fc fragment of human IgG1, linked by an octaglycine spacer. The DNA sequence of the peptibody construct was based on that of Romiplostim, a currently used peptibody for the treatment of immune thrombocytopenic purpura (4–7). The I_{KACh} blocking peptibody was more potent than TP and showed in vivo and in vitro block of I_{KACh}. In patch-clamp experiments, the peptibody was about 300-fold a more potent blocker of I_{KACh} compared to TP. In mice where I_{KACh} activation was via i.p. injection of Cch, the peptibody abrogated the bradycardic consequences of I_{KACh} activation. Moreover, the peptibody decreased the inducibility of AF in aged mice.

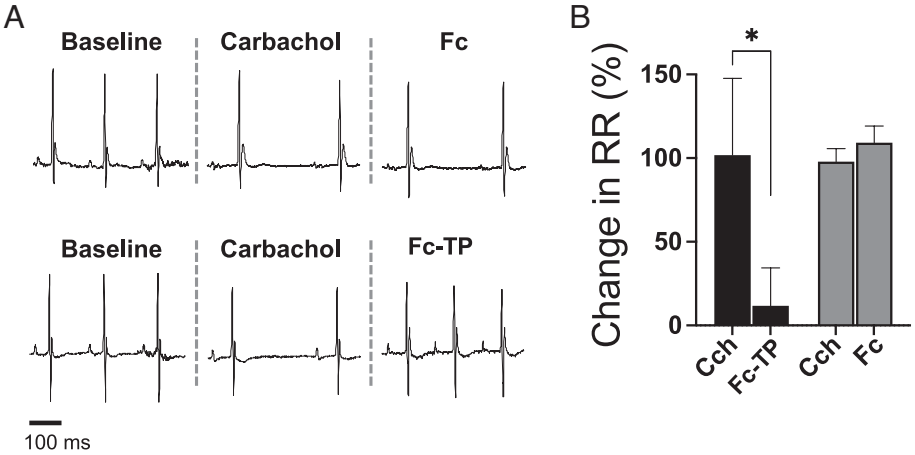

Fig. 5. In vivo block of I_{KACh} in anesthetized mice. *A.* ECG traces in baseline (Ctr), and after i.p. injection of Cch (300 µl of 200 µM), which caused the RR interval prolongation. Jugular vein injection of Fc (*Top*) did not affect the RR, but the peptibody (FcTpQ, *Bottom* trace) shortened the RR back toward baseline. *B.* Percent change in RR interval after Cch injection and then 7 min after administration of Fc (N=6 mice) or FcTpQ (N= 5 mice). *$P < 0.05$, paired Student's *t* test.

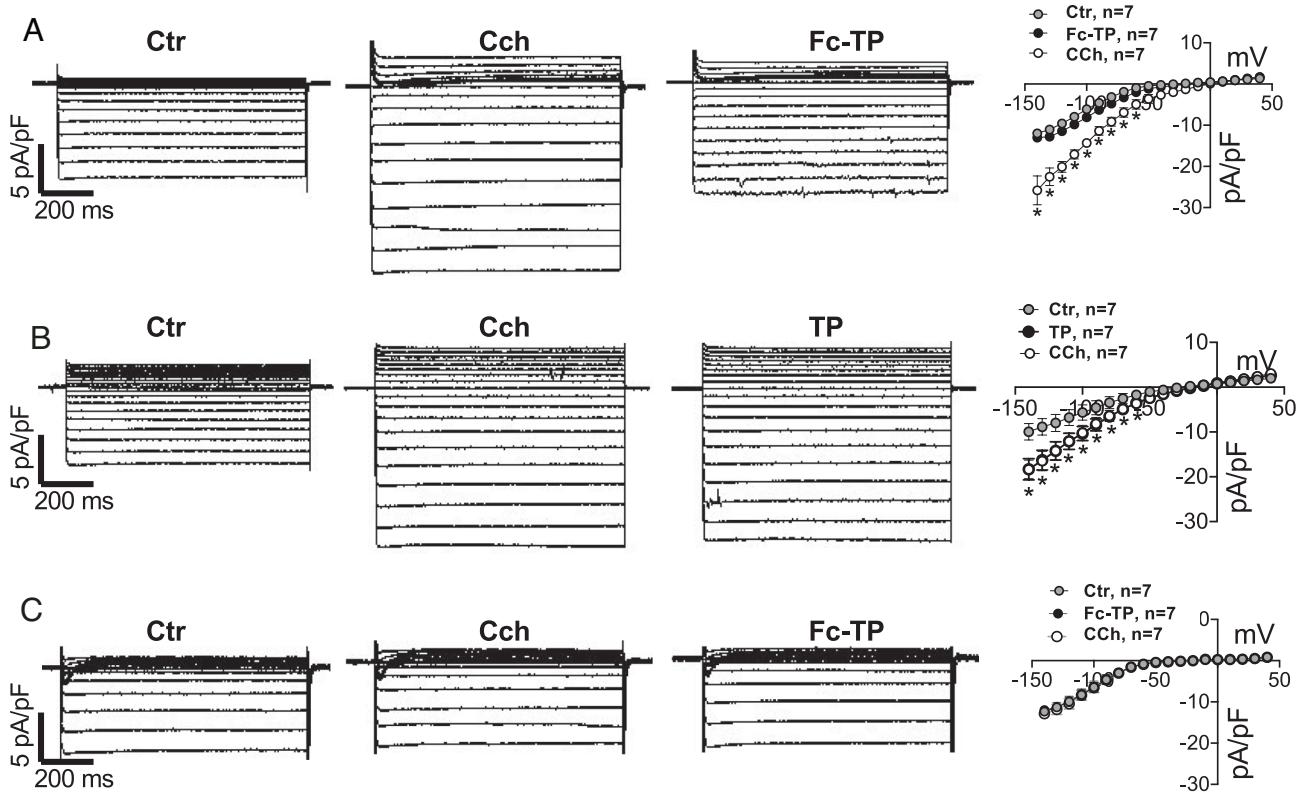

Fig. 6. Atrial specificity of the peptibody. *A.* Ba-sensitive currents in response to voltage steps in an atrial myocyte in control (Ctr), after addition of 10 μM Cch to the bath solution, and after addition of 100 pM peptibody (Fc-TP) to the bath solution in the presence of 10 μM Cch. IV curves show that in atrial myocytes, the Cch current was reduced by application of Fc-TP. *P < 0.05 Cch versus Ctr and Fc-TP, one-way ANOVA, with Bonferroni correction. *B.* Ba-sensitive currents in response to voltage steps in an atrial myocyte in control (Ctr), after addition of 10 μM Cch to the bath solution, and after addition of 100 pM TP to the bath solution in the presence of 10 μM Cch. IV curves show that the Cch current was not reduced by application of TP. *P < 0.05 Cch versus Ctr, and Cch vs. TpQ was not significant, one-way ANOVA, with Bonferroni correction. *C.* Same setup as in *A* and *B*, however in ventricular myocytes. IV curves show that there was no statistically significant difference between Ctr, Cch, and Fc-TP, one-way ANOVA, with Bonferroni correction.

Peptibodies are stable and safe molecules that are shown to be viable therapeutics. Currently, there are two peptibodies in clinical use: Romiplostim for immune thrombocytopenic purpura (5), and Dulaglutide, for glucose control in type 2 diabetes (24, 25). This is in addition to other therapeutic peptibodies in different stages of development (2). The peptibody Romiplostim is composed of thrombopoietin mimetic peptides fused to the C terminus of the Fc fragment of human IgG (2–8). Dulaglutide is a fusion protein consisting of glucagon-like peptide-1 receptor agonist and Fc (24, 25). Such protein chimeras of a biologically active peptide and the Fc domain of IgG are thought to have an extended half-life compared to the biologically active peptide, due to the neonatal Fc receptor salvage pathway involved in protecting IgG from degradation, and decreased renal clearance rate because of the larger size of the peptibody compared to that of the biologically active peptide (2, 3).

Peptibodies may offer an increased avidity to the target compared to the biologically active peptide alone (2, 3). For instance, in the I_{KACh} blocking peptibody (Fig. 1) the homodimerization of the two Fc moieties results in two TP "warheads" per peptibody, and the polyglycine linker which provides flexibility could also result in an increased avidity (2, 3). Interestingly, and although not yet clear why, certain peptides seem to be more active when fused to the carboxy terminus of the Fc; however, in the case of the anti-I_{KACh} peptibody, having the C terminus of TP free is desirable since the C terminus is suggested to be important for the channel blocking activity of the peptidotoxin.

Using homology modeling, molecular docking, and MD simulations, we developed tertiapin-Kir3.1/3.4 and peptibody-Kir3.1/3.4 models and calculated the binding free energies in each system (Figs. 3 and 4). The interactions between the tertiapin moiety and the channel are mainly electrostatic, where several salt-bridge pair interactions were formed and characterized by MD simulations. The critical residues in tertiapin (three C-terminal and one N-terminal positively charged amino acids) interacted with negatively charged Kir3.4 residues E131 and D123. The E131 and D123 residues in Kir3.4 correspond to Kir3.1 residues A125 and V117, respectively. The peptibody bound two Kir3.1/3.4 channels, and the binding free energy of the peptibody-Kir3.1/3.4 complex was about 20 kcal/mol lower than that of tertiapin- Kir3.1/3.4. The lower binding free energy and the double warheads of the peptibody most likely contributed to the higher potency of I_{KACh} block by the peptibody compared to TP (Fig. 2).

From a mechanistic point of view, it has been shown that while I_{KACh} is constitutively active in persistent AF, it is not constitutively active in patients with paroxysmal AF (26). Therefore, we contend that a bioengineered I_{KACh} blocker, which is designed to terminate AF that depends in part on a constitutively active I_{KACh}, would not be useful in paroxysmal AF. Indeed, a large animal model of persistent AF will be needed to evaluate the effects of the Fc-TP peptibody on the arrhythmia, and the time course and dynamics of AF supression or burden modulation.

The gastrointestinal and nervous systems are possible sites for the anti-I_{KACh} peptibody extracardiac toxicity. However, this does not seem likely. For instance, it has been shown that TP does not affect inward rectifier potassium currents in colonic smooth muscle cells and thus contractility of these cells does not seem dependent on I_{KACh} (27). Moreover, since IgG crossing of the blood–brain

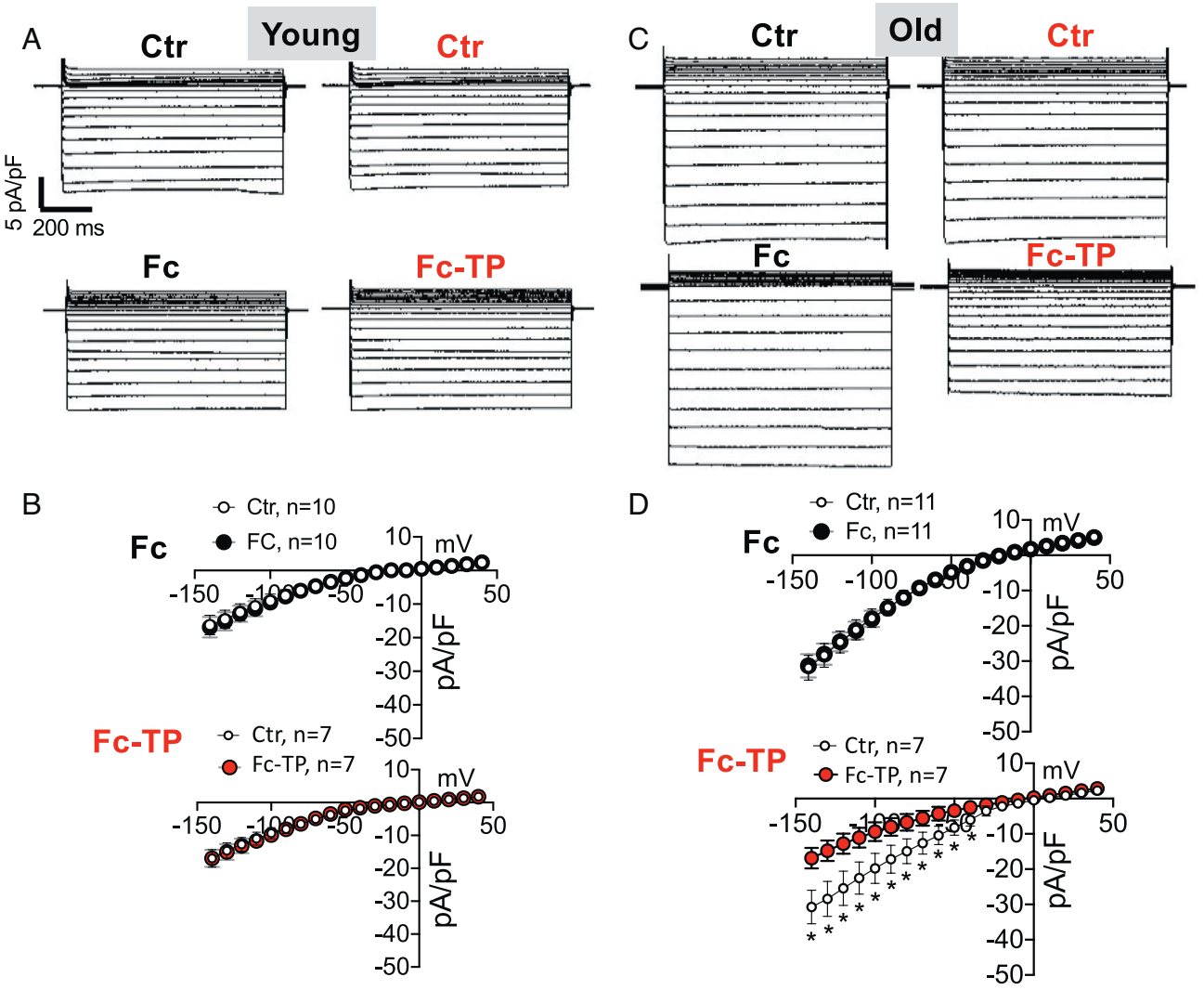

Fig. 7. The peptibody blocks constitutively active I_{KACh} in atrial myocytes from the aged mouse heart. *A.* Ba-sensitive background current tracings from atrial myocytes of young mice. *Top* tracings; baseline control. *Bottom* tracings; after addition of 100 pM Fc fragment (*Left*) or the peptibody (Fc-TP, *Right*). *B.* IV curves of baseline, and Fc (*Top*) and baseline and Fc-TP (*Bottom*). *C.* The top tracings are for baseline control, and the bottom tracings are after addition of 100 pM Fc fragment or the Fc-TP in atrial myocytes from aged mice. The Fc fragment did not affect the current. However, Fc-TP significantly reduced the current. *D.* IV curves of FC (*Top*) and Fc-TP (*Bottom*). *$P < 0.05$, Fc vs. Fc-TP, paired Student's *t* test.

barrier is restricted (28, 29), we expect that the crossing of our peptibody from the blood to the brain to be restricted as well. Interestingly, intracerebral injection of IgG results in the reverse transcytosis of the IgG from brain to blood. (29)

Currently, there are no bioactive peptibodies that could potentially be atrial-selective antiarrhythmics, in the setting of atrial fibrillation. In some forms of AF, I_{KACh} is thought to play a role in the perpetuation of this arrhythmia (1, 16, 17). We and others have shown that blocking I_{KACh} with TP or with the small molecule chloroquine, in animals (30, 31) and patients (22, 30, 32–34), could modulate AF. Therefore, targeting this atrial-specific current with tactics that rely on chimeric proteins of Fc and peptide blockers might offer avenues for pharmacotherapy in atrial fibrillation.

In summary, we demonstrate that engineered peptibodies can be potent and bioactive ion channel blockers. Our peptibody blocks I_{KACh} in vivo and in vitro and can reduce the inducibility of atrial fibrillation. Given that ionic currents such as I_{KACh} could play a role in the perpetuation of arrhythmias including atrial fibrillation, approaches for antiarrhythmic "biobetter" therapies that rely on anti-ion channels peptibody engineering warrant consideration.

Materials and Methods

Animals. Our study conformed with the NIH Guide for the Care and Use of Laboratory Animals and was approved by the Committee on Use and Care of Animals of the University of South Florida. Animals of both sexes were used. C57BL/6J mice of both sexes were used in our experiments.

Peptibody Construct. The DNA sequence of the peptibody (Fc-TP) construct was based on that of Romiplostim (2, 6) and commercially synthesized (Genescript).
Construct. EcoRI-Kozak sequence-Artificial leader sequence-hIgG1FC-Linker-TertiapinQ-Stop codon-HindIII.
Protein Sequence (378 aa). MGWSCIILFLVATATGVHSASTKGPSVFPLAPSSKSTS
GGTAALGCLVKDYFPEPVTVSWNSGALTSGVHTFPAVLQSSGLYSLSSVVTVPSSSLGTQT
YICNVNHKPSNTKVDKKVEPKSCDKTHTCPPCPAPELLGGPSVFLFPPKPKDTLMISRT
PEVTCVVVDVSHEDPEVKFNWYVDGVEVHNAKTKPREEQYNSTYRVVSVL
TVLHQDWLNGKEYKCKVSNKALPAPIEKTISKAKGQPREPQVYTLPPSRDELTKNQVSLTCL
VKGFYPSDIAVEWESNGQPENNYKTTPPVLDSDGSFFLYSKLTVDKSRWQQGNVFSCSVM
HEALHNHYTQKSLSLSPGKGGGGGGGGALCNCNRIIIPHQCWKKCGKK
DNA Sequence. GAATTCCCGCCGCCACCATGGGCTGGTCCTGCATCATTCTGTTTCTGGT
GGTGGCCACAGCCACCGGCGTGCACTCTGCTTCTACAAAGGGCCCTA
GCGTGTTCCCTCTGGCTCCTAGCAGCAAGTCTACAAGCGGAGGAACAGCCGCTCTGG
GCTGCCTGGTCAAGGATTACTTTCCCGAGCCTGTGACCGTGTCCTGGAATAGCGGAGCAC
TGACATCTGGCGTGCACACATTTCCAGCCGTGCTGCAGTCTAGCGGCCTGTACTCTCTGA

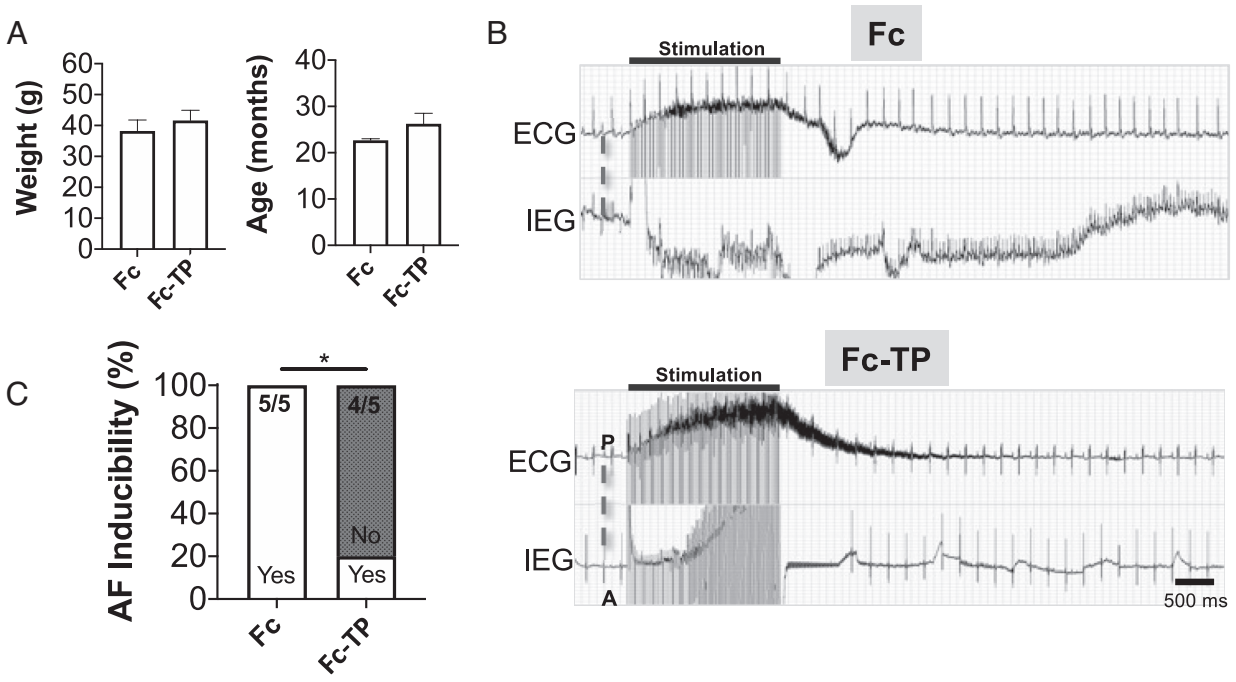

Fig. 8. Antiarrhythmic effects of the peptibody in aged mice. *A.* Weight and age of mice that received Fc or Fc-TP. *B. Top*: ECG (top trace) and intracardiac electrogram (bottom trace) in a mouse after administration of Fc. Two-second burst pacing induced AF. *Bottom*: ECG (top trace) and intracardiac electrogram (bottom trace) in a mouse after administration of Fc-TP. Two-second burst pacing did not induce AF. *C.* Inducibility of AF in five aged animals that received Fc, and in five aged animals that received the peptibody. P * < 0.05, Fisher's exact test.

GCAGCGTGGTCACAGTGCCAAGCTCTAGCCTGGGCACCCAGACCTACAT
CTGCAATGTGAAC CACAAGCCTAGCAACACCAAGGTGGACA
AGAAGGTGGAACCCAAGAGCTGCGACAAGACCCACACCTGTCCTCCATGTCCTG
CTCCAGAACTGCTCGGCGGACCTTCC GTGTTCCTGTTTCCTCCAAAGCC
TAAGGACACCCTGATGATCAGCAGAACCCCTGAAGTGACCTGCGTGGTGGTGGATGT
GTCCCACGAGGATCCCGAAGTGAAGTTCAATTGGTACGTGGACGGCGTGG
AAGTGCACAACGCCAAGACCAAGCCTAGAGAGGAACAGTACAACAGCAC
CTACAGAGTGGTGTCCGTGCTGACAGTGCTGCACCAGGATTGG
CTGAACGGCAAAGAGTACAAGTGCAAGGTGTCCAACAAG
GCCCTGCCTGCTCCTATCGAGAAAACCATCAGCAAGGCCAAGGGCCAGCCTAGGGAA
CCCCAGGTTTACACACTGCCTCCAAGCAGGGACGAGCTGACCA
AGAATCAGGTGTCCCTGACCTGCCTCGTGAAGGGCTTCTACCCTTCCGATATCGCCGTGGA
ATGGGAGAGCAATGGCCAGCCTGAGAACAACTACAAGACA
ACCCCTCCTGTGCTGGACAGCGACGGCTCATTCTTCCTGTACAG
CAAGCTGACCGTGGACAAGTCCAGATGGCAGCAGGGCAACGTGTTCA
GCTGCAGCGTGATGCACGAGGCCCTGCACAACCACTACACCC
AGAAGTCCCTGAGCCTGTCTCCTGGAAAAGGTGGCGGAGGT
GGCGGAGGCGGAGCACTCTGTAATTGCAACCGGATCATTATTCCGCATCAGTGTTGGAA
AAAATGTGGGAAGAAGTGATAAGCTT

Expression and Purification of the Peptibody. The Expi293F cell culture (1L total) was maintained in a 37 °C incubator with ≥80% relative humidity and 8% CO_2 on an orbital shaker platform. One day before transfection, the cells were seeded to a final density of 2.5×10^6 viable cells/mL and allowed to grow overnight. On the day of transfection, the culture was diluted to 3×10^6 viable cells/mL with fresh, pre-warmed Expi293™ Expression Medium. The transfection was performed using ExpiFectamine™ 293 Transfection Kit according to the manufacturer's protocol. In short, peptibody plasmid DNA/Opti-MEM™ and ExpiFectamine™ 293/Opti-MEM™ mixtures were prepared separately and incubated at room temperature for 5 min. Diluted ExpiFectamine™ 293 Reagent was then added to the diluted DNA, and the total complex mixture was incubated at room temperature for another 20 min and then slowly transferred to the cell culture. Eighteen hours post-transfection, ExpiFectamine™ 293 Transfection Enhancer 1 and ExpiFectamine™ 293 Transfection Enhancer 2 were added to the culture. The cell culture supernatant was collected on day 6 and prepared for purification. The peptibody was purified using protein A chromatography (HiTrap rProtein A FF, GE Healthcare) in a 5-ml column pre-equilibrated with PBS. The peptibody was eluted in 0.1 mM acetic acid by fast protein liquid chromatography and immediately buffer-exchanged by dialysis in PBS.

Western Blot. The purified peptibody or recombinant human Fc (Abcam) were then separated by 4 to 15% pre-stained SDS-PAGE Mini-PROTEIN stain-free gel (BIO RAD), transferred to a polyvinylidene difluoride membrane (Merk Millipore), and then probed with biotinylated protein G, 1:10,000 (Thermofisher), and horseradish peroxidase conjugated streptavidin, 1:10,000 (Thermofisher) and imaged with Biorad gel documenting system.

Quantification of the Peptibody Half-Life. Mice received 5.5 μg in 50 μl PBS of the peptibody via tail vein injection. Blood samples were taken by a submandibular bleed at 3 min, 1 h, 3 h, 6 h, 1 d, 3 d, and 7 d. Blood samples were held on ice until clotting occurred, then centrifuged at 13,000 g for 30 min at 4 °C. Quantification of the peptibody in plasma was performed with the human IgG1 Fc ELISA Kit (Aviva Systems). The HRP ELISA assay was conducted as described by the manufacturer's manual, and absorbance was read at 450 nm on a Synergy MX plate reader (BioTeK). Half-life was determined via fitting with a one-phase decay in Prism 8 (GraphPad).

Single-Cell Isolation. Atrial and ventricular myocytes were enzymatically dissociated from C57BL/6J mice of both sexes according to our previous work (35, 36). The excised hearts were retrogradely perfused at 2 ml/min through the aorta at 36.5 °C, for 3 min with Ca^{2+}-free Tyrode solution containing (in mM) 137 NaCl, 5.4 KCl, 10 N-2-hydroxyethylpiperazine-N-2-ethane sulfonic acid (HEPES), 1 $MgCl_2$, and 10 glucose (pH 7.3); then with Ca^{2+}-free Tyrode solution containing 1 mg/ml collagenase Type A (Roche) and 0.08 mg/ml protease Type XIV (Sigma-Aldrich) for 8 to 11 min; and then with Tyrode solution containing 0.2 mM $CaCl_2$ for 5 min. The single cells were obtained by dissociation via gentle agitation of digested atrial or ventricular tissues. Atrial or ventricle myocytes suspensions were filtered through a nylon mesh, and cells were stored at room temperature in Tyrode solution.

Patch Clamp. We used patch clamp to measure the effects of the peptibody, TP, or Fc on I_{KACh} in HEK293 cells stably transfected with Kir3.1 and Kir3.4 (15) and in mouse atrial and ventricular myocytes (35, 36). Currents were recorded using the Multiclamp 700B (Molecular Devices) amplifier an A/D converter (Digidata

1550B plus Hum Silencer, Molecular Devices), and the pClamp 10.6 PC software (Molecular Devices). The analysis was performed with Clampfit 10.6 (pClamp, Molecular Devices) and OriginPro 2018b software packages (OriginLab Corp). Patch pipettes were pulled from glass capillaries (Kimble Glass) and had a resistance of 2.5 to 3 MΩ. After gigaohm seal formation, whole-cell recordings were performed at room temperature. In transfected HEK cells, as previously reported (22), the bath solution contained in mM 90 NaCl, 50 KCl, 1 $CaCl_2$, 2 $MgCl_2$, 10 HEPES, 10 Glucose, and the pH was adjusted to 7.4. The pipette internal solution contained in mM 100 K-aspartate, 10 NaCl, 40 KCl, 5 Mg-ATP, 2 egtazic acid (EGTA), 0.1 GTP-Tris, and 10 HEPES at pH = 7.2. In HEK293 cells, I_{KACh} whole-cell current was elicited by a holding potential at 0 mV for 150 ms followed by steps to −140 mV for 200 ms. Subsequently, the voltage was increased, as a 2-s ramp from −140 mV to +40 mV, followed by a return to 0 mV (22). I_{KACh} was taken as the 1 mM $BaCl_2$-sensitive current. Dose-response curves and IC_{50}s for the block at −120 mV were determined using Prism 8 software (GraphPad). Drops of isolated atrial and ventricular murine myocytes in suspension were applied to the microscope's recording chamber. The extracellular solution was composed of (mM) 100 NaCl, 50 KCl, 1 $MgCl_2$, 5 HEPES, and 5.5 D-glucose, adjusted to pH 7.4. The pipette solution contained: 140 mM KCl, 1 mM $MgCl_2$, 10 mM HEPES, 5 mM EGTA, 5 mM Mg-ATP, and 0.1 mM GTP, pH adjusted to 7.2 with KOH. Whole-cell currents were recorded as described (35, 36) by holding at −40 mV for 100 ms, followed by 1,000 ms steps from −140 mV to +40 mV in 10 mV increments. After recording baseline currents, the extracellular solution was exchanged to contain 20 μM Cch to activate I_{KACh}, followed by application of the peptibody, TP, or Fc. Constitutively active I_{KACh} was measured by application of 100 pM Fc or peptibody to the bath solution, without Cch prestimulation.

In Vivo Electrophysiological Studies in Mice. For measuring the effects of the peptibody on the ECG of mice with Cch injection, mice were anesthetized (1.8% isofluorane), and the exposed right jugular vein instrumented with a PE tube connected to a 250-μL Hamilton syringe for drug delivery. ECG leads were fixed subcutaneously in the Lead II configuration and recorded via Animal Bio Amp (AD Instruments) and digitized via the PowerLab data acquisition system (AD Instruments). LabChart Pro 7.2 software (AD Instruments) was used for acquisition and analysis of the ECG. Continuous ECG was recorded, and mice received an i.p. injection of Cch (300 μl of 200 μM). Five minutes after Cch injection, the peptibody or the Fc fragment was delivered via the jugular vein. For atrial fibrillation inducibility, intracardiac programmed electrical stimulation was performed (37) using a Millar 1.2 French octapolar catheter with an injection port (Millar) placed through the exposed right jugular vein into the right atrium. Intracardiac electrograms and the ECG Lead II were simultaneously recorded using the Advanced Instruments platform. Atrial programmed electrical stimulation was carried out with a stimulus isolator unit (AD Instruments). AF inducibility was performed with 2.5 ms square pulses at twice diastolic threshold in animals injected with the Fc region or the peptibody. The protocol consisted of 2-s trains of burst pacing at 28 to 60 Hz in 2 Hz increments until arrhythmia was induced. Animals showing AF episodes longer than 1 s were considered as inducible for AF.

Computational Methods

Homology Modeling of the Kir3.1/3.4 Heterotetrameric Channel. Homology models for the Kir3.1/3.4 heteromeric channel (two Kir3.1 and two Kir3.4 protein subunits) based on the crystal structure of Kir3.2 (PDBID: 3SYA) were built. A sequence alignment of Kir3.1, Kir3.4, and Kir3.2 was generated using the ClustalW server (http://www.genome.jp/-tools/clustalw/). The MODELER program (38) was then used to generate 10 initial homology models for the Kir3.1/3.4 heterotetrameric channel, based on the Kir3.2 structural template (39). The modeled channel with the best internal DOPE score from the program was subsequently used for modeling the interaction between the Kir3.1/3.4 channel and tertiapin versus the peptibody.

Molecular Docking of Tertiapin into Kir3.1/3.4 Channel. Tertiapin was docked into the *Kir3.1/3.4* model using the Glide program in the Schrodinger software (Schrödinger Inc.). The grid box was defined to cover the turret region with a box size (32 Å × 32 Å × 32 Å). A total of 21 NMR tertiapin structures in the database (PDBID: 1TER) were used for docking simulations. The top-ranked poses of tertiapin within the Kir3.1/3.4 binding site based on XP scores were selected as the predicted binding conformation for each structure. The binding free energies of selected structures were further calculated by the MMGBSA method as described below.

Modeling the Structure of the Peptibody-Kir3.1/3.4 Complex. The tertiapin-Kir3.1/3.4 channel complex selected based on the predicted binding free energy by the MMGBSA calculation was used to build the peptibody-Kir3.1/3.4 complex. The peptibody model was generated by using the I-TASSER website server (https://zhanglab.ccmb.med.umich.edu/I-TASSER/). A template of immunoglobulin heavy chain (PDBID: 1HZH, H chain) was used to generate the homology model of Fc, while the 8G spacer and tertiapin units of the model were generated without using any templates. The tertiapin's sub-structural units in the peptibody were replaced by the predicted docking conformations (PDBID: 1TER) complexed with the Kir3.1/3.4 channel using Discovery studio software (Biovia Corp).

MD Simulations and MMGBSA Binding Free Energy Calculations. The predicted tertiapin *Kir3.1/3.4* and peptibody *Kir3.1/3.4* complexes were immersed in an explicit lipid bilayer of POPC, POPE, POPS, and cholesterol with a molecular ratio of 25:5:5:1 (40) and a water box with dimensions: 131.8 Å × 133.6 Å × 167.5 Å and 205.7 Å × 202.5 Å × 243.5 Å by using the CHARMM-GUI Membrane Builder webserver (http://www.charmm-gui.org/?doc=input/membrane). 150 mM KCl and extra neutralizing Cl^- counter ions were added into the system. The total number of atoms of the two systems were 227,300 and 827,257 for tertiapin-Kir3.1/3.4 and peptibody-Kir3.1/3.4, respectively. The PMEMD.CUDA program in AMBER16 was used to conduct the MD simulations. The MD simulations were performed with periodic boundary conditions to produce isothermal–isobaric ensembles. Long-range electrostatics were calculated using the particle mesh Ewald method (41) with a 10 Å cutoff. Prior to the production runs, energy minimization of the system was carried out. Subsequently, the system was heated from 0 K to 303 K using Langevin dynamics with the collision frequency of 1 ps^{-1}. During the heating, the tertiapin-Kir3.1/3.4 and peptibody-Kir3.1/3.4 complexes were position-restrained using an initial constant force of 500 kcal/mol/$Å^2$, and weakened to 10 kcal/mol/$Å^2$, allowing lipid and water molecules to move freely. Then, the system went through 5 ns equilibrium MD simulations. Finally, a total of 50 to 100 ns production MD simulation was conducted, and coordinates were saved every 100 ps for analysis. The MMGBSA module, which is implemented in Amber16, was utilized to calculate the binding free energy of tertiapin or the peptibody with the Kir3.1/3.4 channel. One hundred frames of structures were extracted from the last 10 ns or 40 ns of the MD simulation trajectories with a time interval of 100 ps for the binding free energy calculations.

Data, Materials, and Software Availability. All study data are included in the main text.

ACKNOWLEDGMENTS. The HEK 293 cells stably transfected with Kir3.1/3.4 were a kind gift from Dr. Douglas Bayliss, University of Virginia. The computations were supported by the ITS (Information Technology Services) Research Computing at Northeastern University. This work was funded in part by National Institutes of Health grants HL138064 to S.F.N and HL059949-25 to D.E.L.

1. D. Calvo, D. Filgueiras-Rama, J. Jalife, Mechanisms and drug development in atrial fibrillation. *Pharmacol. Rev.* **70**, 505–525 (2018).
2. M. Cavaco, M. Castanho, V. Neves, Peptibodies: An elegant solution for a long-standing problem. *Biopolymers*, (2017), 10.1002/bip.23095.
3. G. Shimamoto, C. Gegg, T. Boone, C. Queva, Peptibodies: A flexible alternative format to antibodies. *MAbs* **4**, 586–591 (2012).
4. P. L. McElroy *et al.*, Romiplostim promotes platelet recovery in a mouse model of multicycle chemotherapy-induced thrombocytopenia. *Exp. Hematol.* **43**, 479–487 (2015).
5. G. Molineux, The development of romiplostim for patients with immune thrombocytopenia. *Ann. N. Y. Acad. Sci.* **1222**, 55–63 (2011).
6. G. Molineux, A. Newland, Development of romiplostim for the treatment of patients with chronic immune thrombocytopenia: from bench to bedside. *British J. Haematol.* **150**, 9–20 (2010).
7. J. L. Nichol, AMG 531: an investigational thrombopoiesis-stimulating peptibody. *Pediatr. Blood Cancer* **47**, 723–725 (2006).
8. B. Wang, J. L. Nichol, J. T. Sullivan, Pharmacodynamics and pharmacokinetics of AMG 531, a novel thrombopoietin receptor ligand. *Clin. Pharmacol. Ther.* **76**, 628–638 (2004).
9. M. D. Drici, S. Diochot, C. Terrenoire, G. Romey, M. Lazdunski, The bee venom peptide tertiapin underlines the role of I(KACh) in acetylcholine-induced atrioventricular blocks. *British J. Pharmacol.* **131**, 569–577 (2000).

10. W. Jin, Z. Lu, Synthesis of a stable form of tertiapin: A high-affinity inhibitor for inward-rectifier K+ channels. *Biochemistry* **38**, 14286–14293 (1999).
11. H. Hibino *et al.*, Inwardly rectifying potassium channels: Their structure, function, and physiological roles. *Physiol. Rev.* **90**, 291–366 (2010).
12. D. E. Logothetis, Y. Kurachi, J. Galper, E. J. Neer, D. E. Clapham, The beta gamma subunits of GTP-binding proteins activate the muscarinic K+ channel in heart. *Nature*. **325**, 321–326 (1987).
13. T. Ivanina *et al.*, Mapping the Gbetagamma-binding sites in GIRK1 and GIRK2 subunits of the G protein-activated K+ channel. *J. Biol. Chem.* **278**, 29174–29183 (2003).
14. Y. Kurachi, M. Ishii, Cell signal control of the G protein-gated potassium channel and its subcellular localization. *J. Physiol.* **554**, 285–294 (2004).
15. Q. Lei *et al.*, Activation and inhibition of G protein-coupled inwardly rectifying potassium (Kir3) channels by G protein beta gamma subunits. *Proc. Natl. Acad. Sci. U.S.A.* **97**, 9771–9776 (2000).
16. J. Heijman, J. B. Guichard, D. Dobrev, S. Nattel, Translational challenges in atrial fibrillation. *Circ. Res.* **122**, 752–773 (2018).
17. D. Dobrev *et al.*, The G protein-gated potassium current I(K, ACh) is constitutively active in patients with chronic atrial fibrillation. *Circulation* **112**, 3697–3706 (2005).
18. J. R. Ehrlich, P. Biliczki, S. H. Hohnloser, S. Nattel, Atrial-selective approaches for the treatment of atrial fibrillation. *J. Am. College Cardiol.* **51**, 787–792 (2008).
19. C. A. Doupnik, Venom-derived peptides inhibiting Kir channels: Past, present, and future. *Neuropharmacology* **127**, 161–172 (2017).
20. Y. M. Wang *et al.*, Investigation of the pharmacokinetics of romiplostim in rodents with a focus on the clearance mechanism. *Pharm. Res.* **28**, 1931–1938 (2011).
21. F. Unverdorben *et al.*, Pharmacokinetic properties of IgG and various Fc fusion proteins in mice. *MAbs* **8**, 120–128 (2016).
22. C. Tobon *et al.*, The antimalarial chloroquine reduces the burden of persistent atrial fibrillation. *Front. Pharmacol.* **10**, 1392 (2019).
23. J. Andrade, P. Khairy, D. Dobrev, S. Nattel, The clinical profile and pathophysiology of atrial fibrillation: Relationships among clinical features, epidemiology, and mechanisms. *Circ. Res.* **114**, 1453–1468 (2014).
24. A. Amblee, Dulaglutide for the treatment of type 2 diabetes. *Drugs Today (Barc)* **50**, 277–289 (2014).
25. E. Jimenez-Solem, M. H. Rasmussen, M. Christensen, F. K. Knop, Dulaglutide, a long-acting GLP-1 analog fused with an Fc antibody fragment for the potential treatment of type 2 diabetes. *Curr. Opin. Mol. Ther.* **12**, 790–797 (2010).
26. N. Voigt *et al.*, Differential phosphorylation-dependent regulation of constitutively active and muscarinic receptor-activated IK, ACh channels in patients with chronic atrial fibrillation. *Cardiovasc. Res.* **74**, 426–437 (2007).
27. X. Huang, S. H. Lee, H. Lu, K. M. Sanders, S. D. Koh, Molecular and functional characterization of inwardly rectifying K(+) currents in murine proximal colon. *J. Physiol.* **596**, 379–391 (2018).
28. R. Villasenor *et al.*, Trafficking of endogenous immunoglobulins by endothelial cells at the blood-brain barrier. *Sci. Rep.* **6**, 25658 (2016).
29. F. Schlachetzki, C. Zhu, W. M. Pardridge, Expression of the neonatal Fc receptor (FcRn) at the blood-brain barrier. *J. Neurochem.* **81**, 203–206 (2002).
30. Y. Takemoto *et al.*, Structural basis for the antiarrhythmic blockade of a potassium channel with a small molecule. *FASEB J.* **32**, 1778–1793 (2018).
31. T. J. Cha *et al.*, Kir3-based inward rectifier potassium current: Potential role in atrial tachycardia remodeling effects on atrial repolarization and arrhythmias. *Circulation* **113**, 1730–1737 (2006).
32. S. F. Noujaim *et al.*, Specific residues of the cytoplasmic domains of cardiac inward rectifier potassium channels are effective antifibrillatory targets. *FASEB J.* **24**, 4302–4312 (2010).
33. D. Filgueiras-Rama *et al.*, Chloroquine terminates stretch-induced atrial fibrillation more effectively than flecainide in the sheep heart. *Circ. Arrhythm. Electrophysiol.* **5**, 561–570 (2012).
34. Z. L. Burrell Jr, A. C. Martinez, Chloroquine and hydroxychloroquine in the treatment of cardiac arrhythmias. *N. Engl. J. Med.* **258**, 798–800 (1958).
35. B. Chidipi *et al.*, Enhancement of contraction and L-type Ca(2+) current by murrayafoline-A via protein kinase C in rat ventricular myocytes. *Eur. J. Pharmacol.* **784**, 33–41 (2016).
36. H. J. Park *et al.*, Parasympathetic response in chick myocytes and mouse heart is controlled by SREBP. *J. Clin. Invest.* **118**, 259–271 (2008).
37. M. Rajab *et al.*, Increased inducibility of ventricular tachycardia and decreased heart rate variability in a mouse model for type 1 diabetes: Effect of pravastatin. *Am. J. Physiol. Heart Circ. Physiol.* **305**, H1807–1816 (2013).
38. A. Sali, T. L. Blundell, Comparative protein modelling by satisfaction of spatial restraints. *J. Mol. Biol.* **234**, 779–815 (1993).
39. M. R. Whorton, R. MacKinnon, Crystal structure of the mammalian GIRK2 K+ channel and gating regulation by G proteins, PIP2, and sodium. *Cell* **147**, 199–208 (2011).
40. E. Leal-Pinto, R. D. London, B. A. Knorr, R. G. Abramson, Reconstitution of hepatic uricase in planar lipid bilayer reveals a functional organic anion channel. *J. Membr. Biol.* **146**, 123–132 (1995).
41. T. Darden, D. York, L. Pedersen, Particle mesh Ewald- an N. Log(n) method for Ewald sums in large systems. *J. Chem. Phys.* **98**, 10089 (1993).